Ab Initio Study of the Torsional Motion in Tolane

Dong Xu and Andrew L. Cooksy

November 2006

Publication Number: CSRCR2006-29

COMPUTATIONAL SCIENCE & ENGINEERING

SAN DIEGO STATE UNIVERSITY

Ab Initio Study of the Torsional Motion in Tolane

Dong Xu [a], Andrew L. Cooksy [b,*]

[a] *Computational Science Research Center,*
San Diego State University, 5500 Campanile Drive, San Diego, CA 92182-1245, USA
[b] *Department of Chemistry,*
San Diego State University, 5500 Campanile Drive, San Diego, CA 92182-1030, USA

Abstract

Accurate prediction of the torsional barrier height in tolane is achieved by systematically extrapolating to the Dunning complete basis set limit at MP2 level with a spin-component-scaled correction. The zero-point energy correction is calculated at the B98/cc-pVDZ level based on a benchmark test using the experimental data for benzene. The final calculated barrier height is 202.2 cm^{-1}, in excellent agreement with the observed value. The correct barrier height enables the the vibrational energy levels and other spectroscopic properties to be determined accurately through numerical integration of the torsional Schrödinger equation. This study provides a nearly complete computational solution to the torsional problem in tolane and may aid the exploration of torsional motions in similar molecules.

---

* Corresponding author. Tel: +1 619 594 5571, Fax: +1 619 594 4634
E-mail address: acooksy@sciences.sdsu.edu (A.L. Cooksy)

1. Introduction

A great deal of experimental and theoretical research has been devoted to tolane (diphenylacetylene, ⬡–C≡C–⬡) and its derivatives. Being the elementary framework of the poly(phenylethynylene) (PPE) family, tolane is a molecule of fundamental importance.
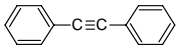
Materials based on tolane and its derivatives have a wide range of applications. Their roles as the traditional building blocks of polymer synthesis [1,2] have been extended to the aromatic core group of the main classes of liquid crystal compounds [3]. The large liquid crystalline phase ranges and high clearing temperatures demonstrated by tolane derivatives contribute to favorable optical behavior when tolane or a related moiety is incorporated into liquid crystalline compounds. In addition, they are used in new metal-containing liquid crystals as ligands for metal-alkyne complexes [4]. A photochemistry study showed the unique structure of tolane moieties results in high thermal stability when homogeneous photoalignment of thin tolane polymer films is induced by light irradiation [5].

Perhaps the most interesting application of tolane and its derivatives is the development of the "π-way" or "molecular wire" like architectures [6-8]. Experiments demonstrate that tolane derivatives with alkyl thiol groups display negative differential resistance (NDR), which is consistent with the concept of substantial "through molecule" conductance that can be influenced by applied potential [9-11]. These systems could be used to store one bit current flow by the torsional motion of the benzene rings [12]. The storage retention time for this class of molecules appears to depend on the specific side groups and their locations [13]. The interaction between the π-conjugated systems and metal d electron systems may lead to an even greater potential for tolane and its derivatives to be used as circuit elements along with nanoparticles and nanotubes in molecular electronics [14].

Applications in molecular electronics have led to new technologies, such as the synthesis of a prototype single-molecule diode [15] and the DNA hairpins in which photoinduced charge transfer is believed to take place through one-dimensional array of π-stacked base pairs in the linked duplex DNA. Substantial interest has been spurred due

to its relevance to oxidative damage and repair [16,17]. Tolane has also received increasing attention in optoelectronics (e.g., organic light emitting diodes, OLED) [18-21].

The origin of many of these developments can be ascribed to the extended linear π-systems of tolane and its derivatives, and consequently to the relative intramolecular orientation of the aromatic rings. The extended π-electron conjugation functions as a natural electrical conductor and the torsional angle(s) between the phenyl rings works as the electric current controller [22]. Tolane, the smallest oligomer, serves as a perfect paradigm for modeling these types of interactions.
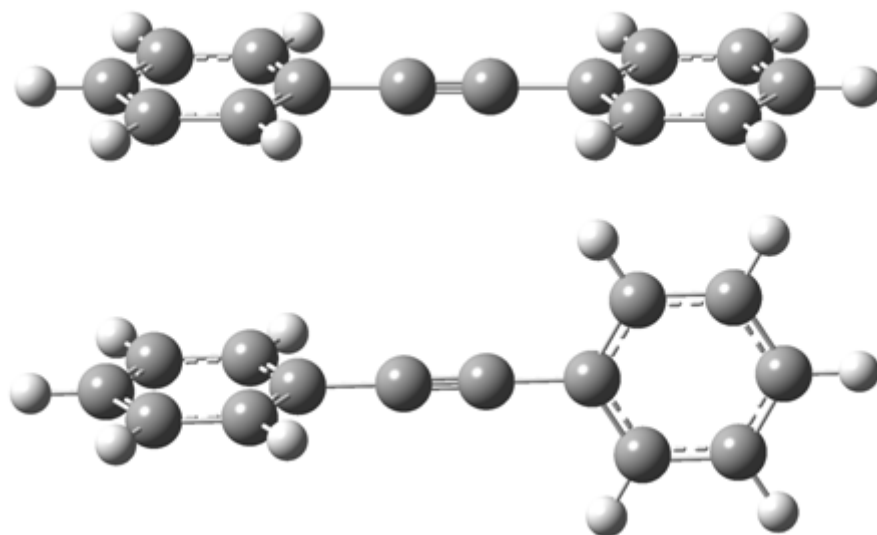
Fig. 1. The coplanar and perpendicular geometries of tolane.

The most thorough experimental study of the torsional motion in tolane was carried out by Okuyama et al. [23] in their single vibronic level fluorescence spectral study using a supersonic free jet. They observed one-photon and two-photon absorption spectra, indicating the presence of inversion symmetry in the molecule, and identified transitions involving levels up to $v = 15$ for the torsional motion. The torsional barrier of 202 cm^{-1} (0.58 kcal mol^{-1}) was then determined with the coplanar configuration of D_{2h} symmetry being the torsional minimum and the perpendicular D_{2d} structure the maximum (Fig. 1).

Many computational studies have investigated the torsional motion in tolane. These include semi-empirical INDO [24] and CNDO [25] calculations, which yielded the opposite conclusion that the perpendicular geometry is more stable than the coplanar

geometry, and a more successful AM1 calculation by Ferrante et al. [26] Recent MM3 calculation found no barrier at all [27]. The small torsional barrier in tolane poses a challenge not only to semi-empirical methods, but also to ab initio calculations because the size of the molecule prohibits the high levels of theory and large basis sets needed for this level of precision. Saebø et al. [28] performed LMP2 calculations with the 6-311G** basis set and obtained a 224 cm^{-1} (0.64 kcal mol^{-1}) barrier height. DFT methods such as B3LYP and B3PW9 were also employed in previous studies. All previously calculated barrier heights and their respective sources are listed in Table 1. The data suggests that appropriate and careful ab initio treatment is required to reproduce the observed torsional barrier.

The current study focuses on the accurate computation of the torsional barrier height in tolane and its vibrational energy levels.

Table 1

Previous computational results for tolane's torsional barrier height

Methods	Barrier Height (cm^{-1})	Barrier Height (kcal mol^{-1})	Source
LMP2/6-311G**	224	0.64	[28]
MP2/6-311G**	128	0.366	[29]
MP2/6-31G*	184	0.53	[30]
HF/6-311G**	148	0.423	[29]
HF/3-21G	147	0.42	[31]
B3LYP/6-31+G*	284	0.81	[27]
B3PW91/6-311G**	301	0.86	[22]
AM1	77	0.22	[26]
MM3	no barrier	no barrier	[27]
INDO	incorrect barrier	incorrect barrier	[24]
CNDO	incorrect barrier	incorrect barrier	[25]
Exp.	202	0.578	[23]

2. Computational Method

2.1. Ab intio PES Determination

All the electronic structure calculations were performed using Gaussian 03 [32]. The coplanar and perpendicular geometries were optimized by at the Hartree-Fock (HF) and second order Møller-Plesset (MP2) [33,34] levels using both Pople-type basis sets [35] (6-31G, 6-311G series) and Dunning's correlation consistent basis sets (cc-pVDZ, cc-pVTZ and cc-pVQZ) [36-38]. To improve efficiency, the initial geometries were first optimized by the HF method with smaller basis sets. All the geometry optimizations were carried out using the Berny algorithm in redundant internal coordinates. Full optimization was requested at coplanar and perpendicular cofigurations. The dihedral angle was frozen to map out the relaxed PES. Use of symmetry was disabled in all calculations.

2.2. SCS-MP2 (Spin-Component-Scaled) Correction

The relatively high computational cost of MP2 and its need for large atomic orbital basis sets to obtain good results are significant deficiencies [39], reducing the upper limit on system size. MP2 also underestimates the contributions from spin-paired electrons, which can result in poor energy prediction. To address these drawbacks, we first applied Grimme's SCS-MP2 correction technique [40] to all the MP2 calculations. Grimme [40] showed that MP2 energies can be systematically improved by separate scaling of the antiparallel-spin (T) and parallel-spin (S) components of the MP2 correlation energy:

$$E_C = E^S + E^T \tag{1}$$

This method was termed "spin-component scaled" MP2, or SCS-MP2, and, denoting the scaling factors as p_S and p_T, the modified correlation energy is simply:

$$E_{C,SCS} = p_S E^S + p_T E^T \tag{2}$$

In this study, Grimme's optimized scaling factors $p_S = 6/5$ and $p_T = 1/3$ were used for antiparallel-spin and parallel-spin (S) correlations. For a given basis set, Grimme's approach showed clear statistical improvements over traditional MP2, in some cases achieving results comparable to QCISD or QCISD(T) quality [40].

2.2. Extrapolation to the Complete Dunning Correlation Consistent Basis Set

The basis set limit of MP2 can be overcome by extrapolating the correlation energies sysmatically to the complete basis set (CBS) limit. We applied the following scheme formulated by Wilson and Dunning [41]:

$$E_{HF}(\infty) = E_{HF}(n) - Ae^{-C \cdot n} \tag{3}$$

where $E_{HF}(\infty)$ is the Hartree-Fock energy for the complete basis set, n represents the cardinal number of the basis set (e.g., $n = 2$ for cc-pVDZ), $E_{HF}(n)$ is the Hartree-Fock energy at the cc-pVnZ basis set, A and C are constants which are determined along with $E_{HF}(\infty)$ via a least-squares fit to $E_{HF}(2)$, $E_{HF}(3)$ and $E_{HF}(4)$.

Next, the antiparallel-spin (T) and parallel-spin (S) contributions of the MP2 correlation energy $E^S(\infty)$ and $E^T(\infty)$ at the complete basis set limit are obtained from the following functional forms:

$$E^S(n) = E^S(\infty) + \frac{B}{(l_{max} + d)^m} \tag{4}$$

$$E^T(n) = E^T(\infty) + \frac{B'}{(l_{max} + d)^m} \quad, \tag{5}$$

where $E^S(n)$ and $E^T(n)$ are the antiparallel-spin (T) and parallel-spin (S) contributions of the MP2 correlation energy at cc-pVnZ basis set, l_{max} is the maximum angular momentum represented in each basis set, d is an angular momentum offset and $m = 3$ or 4. Here we use Dunning's empirical numbers for these parameters: $d = 0$, $m = 4$, $l_{max} = 2$ when $n = 2$ and $l_{max} = 3$ when $n = 3$. Thus, $E^S(\infty)$, $E^T(\infty)$ and the constants B, B' can be calculated using $E^S(2)$, $E^S(3)$, $E^T(2)$ and $E^T(2)$, respectively.

2.3. Calculation of the Torsional Energy Levels

The torsional energy levels and wave functions for the independent twisting modes are solutions of the one-dimensional Schrödinger equation:

$$\left[-\frac{\hbar^2}{2I_{red}} \frac{d^2}{d\phi^2} + V(\phi) \right] \psi(\phi) = E\psi(\phi) \tag{6}$$

where $V(\phi)$ is a periodic potential for the torsional motion and I_{red} is the reduced moment of inertia. Since the rotational constant $B = \hbar/2I_{red}$, the above equation can be written as:

$$\left[-B\frac{d^2}{d\phi^2} + V(\phi) \right]\psi(\phi) = E\psi(\phi) \ . \tag{6}$$

$V(\phi)$ is represented by the following cosine function:

$$V(\phi) = \frac{1}{2}V_2\left(1 - \cos 2\phi\right) \ , \tag{7}$$

where V_2 is the twofold barrier height for the internal rotation. The experimental barrier height 202 cm^{-1} was obtained by fitting the observed spectroscopic transition frequencies to equation (7) [23]. In the current study, we calculate the torsional barrier by applying the ab initio procedures described in *2.1 - 2.3*, the Schrödinger equation was then solved numerically in an effort to provide a computational solution to the tolane torsional problem.

Using a combined numerov process and shooting method [42], the numerical integration of the torsional Schrödinger equation was carried out on 5000 point grids over the range [$\pi/2$, $3\pi/2$] for the torsional angles ϕ, using tolane's rotational constant B = 0.379 cm^{-1} and the barrier height predicted by MP2 calculations with the SCS correction in the Dunning complete basis set limit.

3. Results and Discussion

3.1. Optimized Geometry

All calculations except the HF/6-311++G and HF/6-311++G** correctly predicted the coplanar geometry as the potential energy minimum. An imaginary frequency was found at the optimized geometry when the dihedral angle was fixed top 90°, indicating the perpendicular geometry is a saddle point. These results agree with the experimental findings.

3.2. Torsional Barrier Calculations

The results of preliminary calculations on the torsional barrier as a function of basis set and level are shown in Table 2. HF calculations with Pople-type basis sets show an irrational trend that smaller basis sets produce better results, with diffuse functions leading to the wrong minimum geometry. However, HF results using Dunning's correlation consistent basis sets show that the accuracy improves as the basis set size increases. Next we performed MP2 calculations. The results show improvement over HF results using the same basis set when the SCS correction is applied using the correlation consistent basis set.

After systematically extrapolating to the complete basis set (CBS) limit in combination with SCS-MP2 correction, we obtain a barrier height of 206.2 cm^{-1}, in excellent agreement with Okuyama's analysis. This result demonstrates that the quality of the MP2 calculation can be dramatically improved by applying the SCS-MP2 correction and CBS extrapolation, providing an efficient and effective technique when calculation is limited by computationals resources.

3.2. Zero-point Energy Correction

Table 3 shows the ΔZPEs between the 90° transition state and the 0° energy minimum predicted by different methods using cc-pVDZ basis set. The MP2 calculates a relatively large positive value of 64.8 cm^{-1}for ΔZPE, perhaps for the same reason that uncorrected MP2/cc-pVnZ levels of theory generally overestimate the barrier height. Unfortunately, the SCS-MP2 correction cannot be applied to analytical frequency calculations. In order to better estimate the ΔZPE, we carried out frequency calculations on benzene. The 30 vibrational modes of benzene were compared side by side with the experimental frequencies reported by Goodman et al. [43]. The results are listed in Table

4. The order of accuracy in terms of the total ZPE for benzene is B98 > B3LYP > MP2 > HF. The same order follows when comparing the maximum error among all vibrational modes. B98 leads the pack with only 0.9% error in total ZPE and 3.5% in maximum error across all 30 vibrational modes. The maximum error for MP2 is 12.5%, which is as high as HF. The maximum error comes from mode 19, a C-C bond stretching mode with B_{2u} symmetry. In the MP2 calculation, the frequency at mode 19 is predicted higher than mode 20, an in-plane C-H bond bending mode with A_{2g} symmetry, in clear disagreement with experiment. The same error was also observed by Goodman et al. in their MP2/6-311** calculations [43]. We believe this same effect to some extent explain the discrepancies between MP2 and other ZPE results. Since the perpendicular geometry is generally more rigid than coplanar geometry in tolane, it is expected that the correct ΔZPE has a small negative value. Both DFT results shows the correct sign, -10.8 cm^{-1} from B3LYP and -4.0 cm^{-1} from B98. Based on the good performance of B3LYP and B98 in benzene benchmark test, we believe the B98 ΔZPE (-4.0 cm^{-1}) for tolane is the most reliable value. Beause most of the ZPE scaling factors are very close to 1 and the predicted ΔZPE is small, ZPE scaling does not greatly affect the final barrier height. Thr final value is 202.2 cm^{-1} with B98 ZPE correction, in excellent agreement with the observed barrier height.

3.3. Determination of Torsional Energy Levels
The second goal in this study is to precisely reproduce the experimentally measured torsional vibrational levels. The first column of Table 3 shows the energy levels observed from $v = 0$ to the highest vibrational state observed $v = 15$, which lies near the top of the barrier. The energy levels are represented in the form of energy gaps as a result of the spectroscopy experimental measurement. For even-quantum levels, the values are measured relative to the $v = 0$ state, for odd-quantum levels, the values are measured relative to the $v = 1$ state. The second column is Okuyama et al.'s calculation based on the Hamiltonian matrix diagonalization technique developed by Lewis et al. [44] The third column shows the energy levels calculated by our numerical integration method. The three sets of data are in excellent agreement on all torsional levels. The data also illustrate that the energy levels are doubly degenerate near the bottom of the potential well while the levels split apart near the top of the barrier because of the tunneling

through the barrier. Our solver predicts that the energy splits start from $v = 13$ instead of the lower $v = 12$ level shown by Okuyama's simulation. Our solver is also able to predict higher energy levels as well as $v = 0$ and $v = 1$ levels, which are not directly available from the experiment [23]. This determines the fundamental frequency for ground state tolane to be 17.4 cm^{-1}. The final potential energy curve and torsional energy levels are plotted in Fig 2.

Table 2

Calculation results for tolane torsional barrier height

Methods	Barrier (cm^{-1})	SCS-MP2 Barrier (cm^{-1})
HF/6-31G	169.1	
HF/6-31G*	152.2	
HF/6-31G**	151.0	
HF/6-311G**	142.7	
HF/6-311++G	-190.8	
HF/6-311++G**	-11.4	
MP2/6-31G	31.4	39.8
MP2/6-31G*	170.4	140.8
MP2/6-31G**	176.9	147.4
MP2/6-311G**	170.8	139.3
MP2/6-311++G	222.9	118.6
MP2/6-311++G**	186.7	127.5
HF/cc-pVDZ	151.7	
HF/cc-pVTZ	154.9	
HF/cc-pVQZ	161.6	
HF/CBS	167.4	
MP2/cc-pVDZ	223.6	183.1
MP2/cc-pVTZ	237.5	192.3
MP2/CBS	252.6	**206.2**
Exp.	**202.0**	

Table 3

Benzene frequency calculation benchmark test[a]

Mode	Symmetry	Exp.	mp2 /cc- pVDZ	Error(%)	HF /cc- pVDZ	Error(%)	B3LYP /cc- pVDZ	Error(%)	B98 /cc-pVDZ	Error(%)
1	E(2u)	398	400.9	0.7	449.8	13.0	414.1	4.1	411.5	3.4
2	E(2u)	398	400.9	0.7	449.8	13.0	414.8	4.2	412.0	3.5
3	E(2g)	607.2	605.6	-0.3	660.8	8.8	617.7	1.7	614.8	1.3
4	E(2g)	607.2	605.6	-0.3	660.8	8.8	617.8	1.7	615.4	1.4
5	A(2u)	674	633.9	-6.0	752.2	11.6	690.5	2.4	690.5	2.5
6	B(2g)	707	686.0	-3.0	771.3	9.1	723.1	2.3	719.1	1.7
7	E(1g)	847.1	858.9	1.4	948.3	12.0	865.5	2.2	863.7	2.0
8	E(1g)	847.1	858.9	1.4	948.3	12.0	865.8	2.2	864.1	2.0
9	E(2u)	967	953.7	-1.4	1080.7	11.8	986.6	2.0	984.1	1.8
10	E(2u)	967	953.7	-1.4	1085.8	12.3	986.7	2.0	984.3	1.8
11	B(2g)	990	961.9	-2.8	1089.9	10.1	1013.6	2.4	1010.5	2.1
12	A(1g)	994.4	1007.0	1.3	1089.9	9.6	1018.6	2.4	1014.3	2.0
13	B(1u)	1010	1017.0	0.7	1116.5	10.5	1021.9	1.2	1016.6	0.7
14	E(1u)	1038.3	1061.3	2.2	1130.7	8.9	1058.4	1.9	1056.3	1.7
15	E(1u)	1038.3	1061.3	2.2	1130.7	8.9	1058.8	2.0	1056.6	1.8
16	B(2u)	1149.7	1163.1	1.2	1188.2	3.3	1161.9	1.1	1160.1	0.9
17	E(2g)	1177.8	1190.7	1.1	1273.0	8.1	1186.3	0.7	1185.3	0.6
18	E(2g)	1177.8	1190.7	1.1	1273.0	8.1	1186.5	0.7	1185.6	0.7
19	B(2u)	1309.4	1472.4	12.5	1341.0	2.4	1355.6	3.5	1352.1	3.3
20	A(2g)	1367	1358.9	-0.6	1477.4	8.1	1364.1	-0.2	1360.3	-0.5
21	E(1u)	1494	1504.9	0.7	1626.9	8.9	1506.1	0.8	1502.5	0.6
22	E(1u)	1494	1505.0	0.7	1627.0	8.9	1506.5	0.8	1502.7	0.6
23	E(2g)	1607	1649.7	2.7	1787.3	11.2	1644.6	2.3	1640.7	2.1
24	E(2g)	1607	1649.7	2.7	1787.3	11.2	1645.0	2.4	1641.5	2.1
25	B(1u)	3166.3	3209.4	1.4	3328.8	5.1	3166.3	0.0	3163.5	-0.1
26	E(2g)	3174	3220.5	1.5	3340.6	5.2	3176.4	0.1	3173.8	0.0
27	E(2g)	3174	3220.5	1.5	3340.6	5.2	3176.6	0.1	3174.0	0.0
28	E(1u)	3181.1	3236.9	1.8	3359.8	5.6	3192.8	0.4	3190.3	0.3
29	E(1u)	3181.1	3236.9	1.8	3359.8	5.6	3193.0	0.4	3190.6	0.3
30	A(1g)	3191	3246.8	1.8	3371.8	5.7	3203.6	0.4	3201.1	0.3
ZPE		21770.9	22061.3	1.3	23424.1	7.6	22009.7	1.1	21968.9	0.9
Max. Error				12.5		13.0		4.2		3.5

[a]Frequencies are in cm^{-1}.

Table 4

Observed and calculated torsional levels of tolane (cm^{-1})

v	$\Delta v(v-1)$ and $\Delta v(v-0)$		
	Obsvd.[a]	Okuyama et al.[a]	Calc.
0			**8.7**
1			**25.8**
2	34	33.9	33.8
3	33	33.0	33.0
4	66	66.0	66.0
5	65	64.3	64.3
6	97	96.3	96.3
7	94	93.6	93.7
8	125	124.6	124.7
9	121	120.8	120.9
10	150	150.6	150.7
11	144	145.4	145.5
12	173	173.4/173.6	173.6
13	164	165.9/166.9	166.0/166.8
14	189	190.5/193.8	190.6/193.8
15	177	179.8/186.7	179.8/186.7

[a]Reference [23]
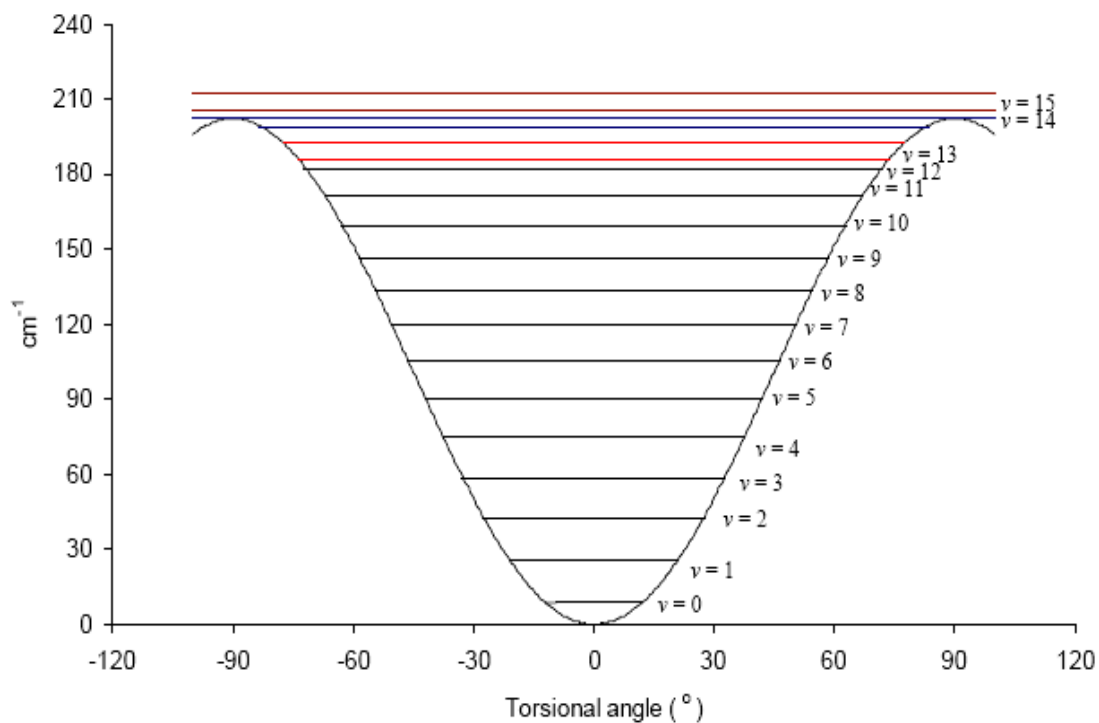
Fig. 2. The tolane torsional barrier and energy levels. The quantum states are doubly degenerate for $v \leq 12$, but split for $v \geq 13$.

4. Conclusion

A nearly complete computational solution to the torsional motion problem in the tolane molecule is presented in this study. Combining the Dunning complete basis set extrapolation technique [41] with the SCS-MP2 correction [40], the torsional barrier height is predicted to high accuracy. Frequency benchmark calculations on benzene were used to predict the zero-point energy correction for tolane. A subsequent numerical solution to the torsional Schrödinger equation over the computed PES reproduces the experimental vibrational energy levels and other spectroscopic properties, some of which are unavailable from experiments. The computational results are in excellent agreement with the observed data. This work demonstrates the effectiveness of using computational tools to treat large amplitude vibrational problems such as the torsional motion in tolane.

Acknowledgements

References

[1]   K.S. Cook, W.E. Piers, R. Mcdonald, J. Am. Chem. Soc., 124 (2002) 5411.
[2]   S. Merlet, M. Birau, Z.Y. Wang, Org. Lett., 4 (2002) 2157.
[3]   D.J. Dyer, V.Y. Lee, R.J. Twieg, Liq. Cryst., 24 (1998) 271.
[4]   D.D. Young, E. Scharrer, M.V. Yoa, Mol. Cryst. Liq. Cryst., 408 (2004) 21.
[5]   C. Mater, S.Y. Morino, K. Ichimura, Chem. Mater, 11 (1999) 1293.
[6]   C. Hortholary, C. Coudret, J. Org. Chem., 68 (2003) 2167.
[7]   J.S. Yang, T.M. Swager, J. Am. Chem. Soc, 120 (1998) 864.
[8]   C.R. Hess, G.A. Juda, D.M. Dooley, R.N. Amii, M.G. Hill, J.R. Winkler, H.B. Gray, J. Am. Chem. Soc, 125 (2003) 7156.
[9]   L.A. Bumm, J.J. Arnold, M.T. Cygan, T.D. Dunbar, T.P. Burgin, L. Jones, Science, 271 (1996) 1705.
[10]   J.M. Seminario, P.A. Derosa, J.L. Bastos, J. Am. Chem. Soc., 124 (2002) 10266.
[11]   Z.J. Donhauser, B.A. Mantooth, K.F. Kelly, L.A. Bumm, J.D. Monnell, J.J. Stapleton, D.W. Price Jr, A.M. Rawlett, D.L. Allara, J.M. Tour, Science, 292 (2001) 2303.
[12]   M.A. Reed, J. Chen, A.M. Rawlett, D.W. Price, J.M. Tour, Appl. Phys. Lett., 78 (2001) 3735.
[13]   C. Li, D. Zhang, X. Liu, S. Han, T. Tang, C. Zhou, W. Fan, J. Koehne, J. Han, M. Meyyappan, Appl. Phys. Lett., 82 (2003) 645.
[14]   S. Ami, M. Hliwa, C. Joachim, Nanotechnology, 14 (2003) 283.
[15]   M. Elbing, R. Ochs, M. Koentopp, M. Fischer, C. Von Hanisch, F. Weigend, F. Evers, H.B. Weber, M. Mayor, Proc. Natl. Acad. Sci. U S A, 102 (2005) 8815.
[16]   F.D. Lewis, T. Wu, X. Liu, R.L. Letsinger, S.R. Greenfield, S.E. Miller, M.R. Wasielewski, J. Am. Chem. Soc., 122 (2000) 2889.
[17]   F.D. Lewis, R.L. Letsinger, M.R. Wasielewski, Acc. Chem. Res., 34 (2001) 159.
[18]   H. Reisch, U. Wiesler, U. Scherf, N. Tuytuylkov, Macromolecules, 29 (1996) 8204.
[19]   M. Ranger, D. Rondeau, M. Leclerc, Macromolecules, 30 (1997) 7686.
[20]   S. Inaoka, R. Advincula, Macromolecules, 35 (2002) 2426.
[21]   S. Merlet, M. Birau, Z.Y. Wang, Org. Lett., 4 (2002) 2157.
[22]   J.M. Seminario, A.G. Zacarias, J.M. Tour, J. Am. Chem. Soc., 120 (1998) 3970.
[23]   K. Okuyama, T. Hasegawa, M. Ito, N. Mikami, J. Phys. Chem., 88 (1984) 1711.
[24]   A. Liberles, B. Matlosz, J. Org. Chem., 36 (1971) 2710.
[25]   A. Mavridis, I. Moustakali-Mavridis, Acta. Cryst., 33 (1977) 3612.
[26]   C. Ferrante, U. Kensy, B. Dick, J. Phys. Chem., 97 (1993) 13457.
[27]   A. Goeller, E. Klemm, D.A.M. Egbe, Int. J. Quantum Chem., 84 (2001) 86.
[28]   S. Saebø, J.E. Almlöf, J.G. Stark, J.E. Boggs, J. Mol. Struct., 200 (1989) 361.
[29]   Y. Shimoi, B.A. Friedman, Nonlinear Optics, 26 (2000) 169.
[30]   A. Borodin, M. Yamazaki, N. Kishimoto, K. Ohno, J. Phys. Chem. A, 110 (2006) 1783.
[31]   S. Anand, O. Varnavski, J.A. Marsden, M.M. Haley, H.B. Schlegel, T. Goodson Iii, J. Phys. Chem. A, 110 (2006) 1305.

[32]   M.J. Frisch, G.W. Trucks, H.B. Schlegel, G.E. Scuseria, M.A. Robb, J.R. Cheeseman, J.A. Montgomery Jr, T. Vreven, K.N. Kudin, J.C. Burant, Gaussian Inc.: Wallingford, CT (2004).

[33]   C. Møller, M.S. Plesset, Phys. Rev., 46 (1934) 618.

[34]   R. Krishnan, J.A. Pople, Int. J. Quantum Chem., 14 (1978) 91.

[35]   J.A. Pople, P.V.R. Schleyer, L. Radom, W.J. Hehre, Ab Initio Molecular Orbital Theory, Wiley, New York, 1986.

[36]   D.E. Woon, T.H. Dunning Jr, J. Chem. Phys., 98 (1993) 1358.

[37]   R.A. Kendall, T.H. Dunning Jr, R.J. Harrison, J. Chem. Phys., 96 (1992) 6796.

[38]   T.H. Dunning Jr, J. Chem. Phys., 90 (2006) 1007.

[39]   T. Helgaker, W. Klopper, H. Koch, J. Noga, J. Chem. Phys., 106 (1997) 9639.

[40]   S. Grimme, J. Chem. Phys., 118 (2003) 9095.

[41]   A.K. Wilson, T.H. Dunning Jr, J. Chem. Phys., 106 (2006) 8718.

[42]   P.C. Chow, Am. J. Phys., 40 (1972) 730.

[43]   L. Goodman, A.G. Ozkabak, S.N. Thakur, J. Phys. Chem., 95 (1991) 9044.

[44]   J.D. Lewis, J.T.B. Malloy, T.H. Chao, J. Laane, J. Mol. Struct., 12 (1972) 427.